

## Article

# Flammability Properties of the Pyrolysis Gas Generated from Willow Wood

Maria Mitu <sup>1,\*</sup> , Domnina Razus <sup>1</sup> , Dorin Boldor <sup>2</sup>  and Cosmin Marculescu <sup>3</sup>

<sup>1</sup> “Ilie Murgulescu” Institute of Physical Chemistry of the Romanian Academy, 202 Splaiul Independentei, 060021 Bucharest, Romania; drazus@icf.ro

<sup>2</sup> Department of Biological and Agricultural Engineering, Louisiana State University Agricultural Center, 149 E. B. Doran, Baton Rouge, LA 70803-4505, USA; dboldor@agcenter.lsu.edu

<sup>3</sup> Department of Energy Production and Use, University Politehnica of Bucharest, 313 Splaiul Independentei, 060042 Bucharest, Romania; cosminmarcul@yahoo.co.uk

\* Correspondence: maria\_mitu@icf.ro

**Abstract:** Willow wood presents a real interest for biomass pyrolysis due to its fast growth, renewability, and high energy density. Following the pyrolysis of willow wood in an inert atmosphere, a multi-fuel gaseous mixture was obtained, with the following composition (by volume): 38.20% CO/21.87% H<sub>2</sub>/17.44% CH<sub>4</sub>/1.15% O<sub>2</sub>/17.15% CO<sub>2</sub>/4.19% N<sub>2</sub>. The propagation of laminar premixed flames in these *multifuel* mixtures with air was investigated numerically for initial temperatures from 298 to 500 K, initial pressures from 1 to 20 bar, and fuel equivalence ratios between 0.60 and 2.00. The combustion of these gaseous mixtures as free laminar premixed flames was simulated by means of the INSFLA package and an extended reaction mechanism with 592 elementary reactions and 53 species. The modelling of the gas-phase combustion delivered several important parameters: the laminar burning velocities,  $S_{li}$ , the maximum flame temperatures,  $T_{fl,max}$ , the flame front thicknesses,  $d_{fl}$ , and the peak concentrations of the main reaction intermediates. The obtained parameters, discussed in correlation with the initial pressure and temperature, afforded the determination of the overall activation parameters of *multifuel* oxidation with air.

**Keywords:** multifuel; laminar burning velocity; flame temperature; flame front thickness



**Citation:** Mitu, M.; Razus, D.; Boldor, D.; Marculescu, C. Flammability Properties of the Pyrolysis Gas Generated from Willow Wood. *Processes* **2023**, *11*, 2103. <https://doi.org/10.3390/pr11072103>

Academic Editor: Chi-Min Shu

Received: 12 June 2023

Revised: 5 July 2023

Accepted: 11 July 2023

Published: 14 July 2023



**Copyright:** © 2023 by the authors. Licensee MDPI, Basel, Switzerland. This article is an open access article distributed under the terms and conditions of the Creative Commons Attribution (CC BY) license (<https://creativecommons.org/licenses/by/4.0/>).

## 1. Introduction

Willow wood is an excellent choice for biomass pyrolysis due to its fast growth, renewability, and high energy density. This process involves heating the willow wood to high temperatures in an oxygen-free environment, often an inert atmosphere, leading to the thermal decomposition of the wood and the generation of solid, liquid, and gaseous biofuels. Biochar (the solid product) is a carbon-rich material that can enhance soil fertility, while bio-oil (the liquid product) is a dark brown liquid that can be utilized as a fuel or chemical feedstock. The gaseous product is a mixture of carbon monoxide, hydrogen (known also as syngas), and other gases that can be employed as a fuel for power generation or as a chemical feedstock. The composition of this gaseous product varies considerably depending on the pyrolysis conditions and the feedstock type [1].

The use of biofuels as alternative energy sources has been increasing in recent years, as they are seen as a more sustainable and environmentally friendly alternative to traditional fossil fuels. However, the use of complex fuel mixtures in power generation, automotive industries, and aviation transportation raises concerns about the chemical and safety aspects of their combustion. As a result, researchers have been focusing more on the study of the safety aspects of complex fuel mixtures.

A key parameter that is of particular interest in the design of industrial processes is the laminar burning velocity ( $S_{li}$ ). This parameter condenses several pieces of information about the reactivity and the exothermicity of the system, which are critical factors in

ensuring the safe and efficient use of these alternative fuels [2]. The laminar burning velocity is a measure of the rate at which a flame front travels through a combustible mixture in the absence of turbulence. This parameter is essential for designing and optimizing combustion processes, as it influences the rate of energy release, the flame stability, and pollutant emissions. Therefore, the laminar burning velocity is a critical parameter for the design of industrial processes, as it helps to ensure that the combustion process is both efficient and safe.

There is a wealth of burning velocity information in the literature, which includes data obtained from simulations as well as experimental studies involving various fuels under different operating conditions. The experimental studies can be divided into two groups. The first group includes measurements conducted on stationary flames, such as Bunsen burners, or a derivative of that method. The second group involves measurements conducted on non-stationary flames in tubes, and later in low-aspect closed vessels. Regardless of the techniques employed, numerous studies have been conducted on CH<sub>4</sub> [3–5] and CH<sub>4</sub>/H<sub>2</sub> [6–8], on binary mixtures such as CH<sub>4</sub>/CO [9], natural gas/H<sub>2</sub> [8], and CO/H<sub>2</sub> [10–14], and on ternary mixtures [15]. Experimental laminar burning velocity data for multi-fuels with four components (CO/CO<sub>2</sub>/H<sub>2</sub>/N<sub>2</sub>) have been provided by Varghese and Kumar [16], and those with five components (H<sub>2</sub>/CO/CO<sub>2</sub>/CH<sub>4</sub>/N<sub>2</sub>) have been provided by Oliveira et al. [17].

Studies on the laminar burning velocity of mixtures that may have in their composition some of H<sub>2</sub>/CO/CH<sub>4</sub>/O<sub>2</sub>/N<sub>2</sub>/CO<sub>2</sub> at variable concentrations are presented in the literature by Di Benedetto et al., Kobayashi et al., Basco et al., Francisco et al., and Zhang et al. [18–23], and studies on the laminar burning velocity of liquid fuels obtained from the pyrolysis of biomass (e.g., rice husk) at high initial pressures and temperatures are presented by Xu et al. [24,25]. From the study by Di Benedetto et al. [18] on CH<sub>4</sub>/O<sub>2</sub>/N<sub>2</sub>/CO<sub>2</sub> and H<sub>2</sub>/O<sub>2</sub>/N<sub>2</sub>/CO<sub>2</sub> mixtures, it was observed that the presence of CO<sub>2</sub> has a strong influence on the whole process, through the specific heat of the mixtures (leading to a decrease in the flame temperature and burning velocity) and through the chemical kinetics of the process. A study on the fuel composition and initial pressure influences on the laminar flame speed of H<sub>2</sub>/CO/CH<sub>4</sub> bio-syngas was presented by Zhou et al. [26].

Earlier research has indicated that the laminar burning velocity of syngas in air is notably affected by the presence of hydrogen in the fuel mixture, owing to its superior laminar burning velocity when combusted with air in comparison to conventional gaseous fuels [27,28]. Furthermore, the introduction of diluents, such as nitrogen and carbon dioxide, to the fuel mixture can significantly reduce the laminar burning velocity due to the inerting properties of these gases [28–30]. A study about explosions of syngas/CO<sub>2</sub> mixtures in oxygen-enriched air was presented by Salzano et al. [31].

The aim of the present paper is to calculate the laminar burning velocities at various initial conditions (temperature, pressure, and composition) for *multifuels* obtained from the pyrolysis process of willow wood (temperature of the pyrolysis process: 800 °C). The experiments were carried out in a fed-batch reactor under nitrogen atmosphere. The data referring to experimental pyrolysis methods applied to the current research study have already been detailed by Ionescu et al. [32]. Therefore, here, only the obtained results concerning the gaseous phase (obtained following the process of the pyrolysis of willow wood at a temperature of 800 °C) will be presented and discussed. The work focuses mainly on the gas resulting from pyrolysis. The composition of the gaseous mixture obtained by the pyrolysis processes of willow wood, experimentally determined by GC, is the following: [CO] = 38.20 vol%; [H<sub>2</sub>] = 21.87 vol%; [CH<sub>4</sub>] = 17.44 vol%; [O<sub>2</sub>] = 1.15 vol%; [CO<sub>2</sub>] = 17.15 vol%; and [N<sub>2</sub>] = 4.19 vol%. Along with these, other components were observed in very small concentrations, which were neglected. In the paper, this mixture was named: “*multifuel A*”. Other *multifuels* obtained by willow wood pyrolysis have close compositions in relation to *multifuel A*, so their behavior was not considered of interest for the present paper.

## 2. Computing Program and Methodology

The laminar burning velocities characteristic for the free laminar premixed flames of gaseous mixtures was computed by the package INSFLA, developed by Warnatz, Maas, and coworkers [33–35], for the simulation of flame propagation in fuel–air mixtures, under various conditions. The present case examined premixed laminar free flames under radiative energy losses. The mechanism CH4-C4, using 53 chemical species which participate in 592 elementary reactions [34], was run, using updated values of several rate coefficients for rate-limiting reactions of propane–air oxidation, as given by Heghes [36]. The runs were performed for the combustion of the *multifuel* (a mixture named *multifuel A*) with air at various initial pressures from 1 bar to 20 bar and various initial temperatures from 298 K to 500 K. As input data, the thermochemical properties of chemical species, as given in [37], were used; their transport coefficients were calculated according to [35].

## 3. Results and Discussion

The results of calculations delivered by the INSFLA package on premixed laminar flames of *multifuel A* with air, at different initial conditions (concentration, pressure, temperature), taking into account radiative losses, are shown in Figures 1 and 2. The data were plotted against the equivalence ratio,  $\varphi$ , defined as:

$$\varphi = \frac{[\text{fuel}]}{[\text{oxygen}]} / \left( \frac{[\text{fuel}]}{[\text{oxygen}]} \right)_{\text{st}} \quad (1)$$

where the index “st” refers to a stoichiometric mixture, whose components (fuel (*multifuel A*) and oxygen) burn completely to CO<sub>2</sub> and H<sub>2</sub>O.

Figure 1 shows the influence of the initial temperature,  $T_0$ , and equivalence ratio,  $\varphi$ , on: (a) laminar burning velocities,  $S_u$ , (b) the flame temperature,  $T_{fl,max}$ , and (c) the flame front thickness,  $d_{fl}$ , of the mixture between *multifuel A* and air at  $p_0 = 1$  bar, while Figure 2 shows the influence of the initial pressure,  $p_0$ , and equivalence ratio,  $\varphi$ , on: (a) laminar burning velocities,  $S_u$ , (b) the flame temperature,  $T_{fl,max}$ , and (c) the flame front thickness,  $d_{fl}$ , of the same mixture at  $T_0 = 298$  K.

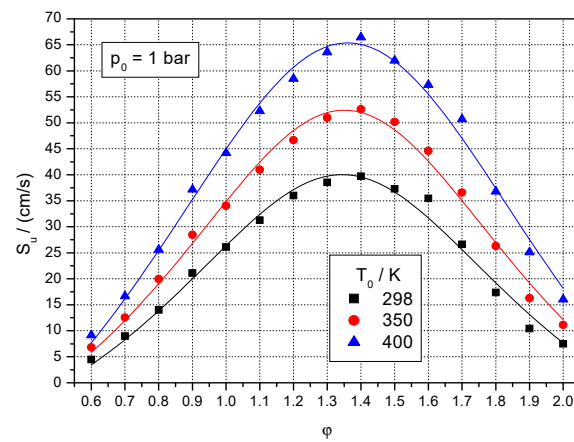
The normal burning velocity is influenced by the initial conditions of the flammable mixture (concentration, temperature, and pressure). The peak burning velocity  $S_{u,max}$  was obtained at the same composition ( $(\text{multifuel A}) = 30.1\text{--}31.6$  vol%;  $\varphi = 1.30\text{--}1.40$ ) for all initial temperatures and/or pressures. The variation in the burning velocity of *multifuel A* with air, at different concentrations, pressures, and initial temperatures, can be seen in Figures 1a and 2a. As the initial pressure increases, a decrease in the burning velocities is observed, and as the initial temperature increases, an increase in the burning velocities is observed.

The variation in the maximum temperatures in the flame front  $T_{fl,max}$ , as a function of the concentration of the studied mixture in air at different initial pressures and temperatures, is represented in Figures 1b and 2b. It can be observed that the maximum temperature in the flame front,  $T_{fl,max}$ , reaches the highest value in the field of the most reactive mixtures close to the equivalence ratio  $\varphi = 1.10$ . The values of maximum temperatures in the flame front register higher values with the increase in the initial pressure, while the initial temperature has a less significant influence on  $T_{fl,max}$ .

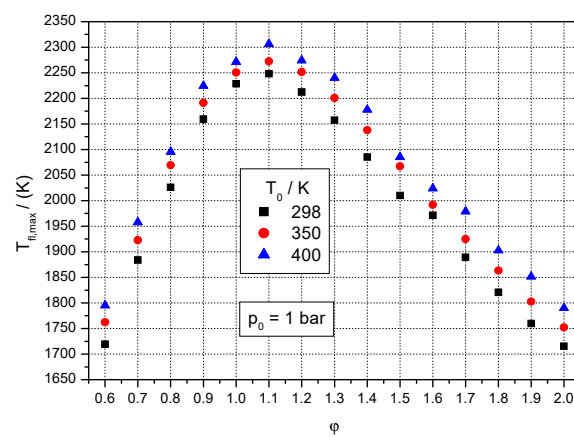
In Figure 1b, the ratio  $(T_{fl,max})_{400\text{ K}} / (T_{fl,max})_{298\text{ K}}$  was 1.019 for the stoichiometric mixture. In Figure 2b, the ratio  $(T_{fl,max})_{10\text{ bar}} / (T_{fl,max})_{1\text{ bar}}$  was 1.016 for the same mixture.

Similar to the burning velocity and the flame temperature, the flame front thickness,  $d_{fl}$ , depends on the initial conditions of the flammable mixture (concentration, temperature, and pressure). The variation in the flame front thickness as a function of the initial temperature at different initial pressures of *multifuel A* with air at different equivalence ratios is represented in Figures 1c and 2c. The lowest values of the flame front thickness  $d_{fl}$  are observed in the range of rich mixtures ( $\varphi = 1.30\text{--}1.40$ ) depending on the initial pressure. With the increase in the initial pressure, a decrease in the values of the flame front thickness is observed, and the same behavior is also found in the case of an increase in the

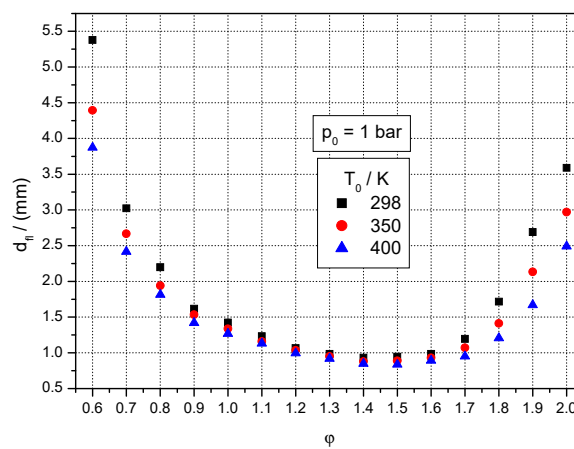
initial temperatures, i.e., the thickness of the flame front decreases with the increase in the initial temperature.



(a)

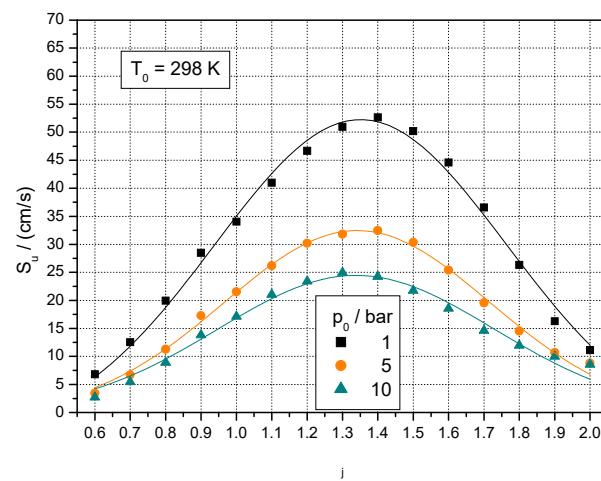


(b)

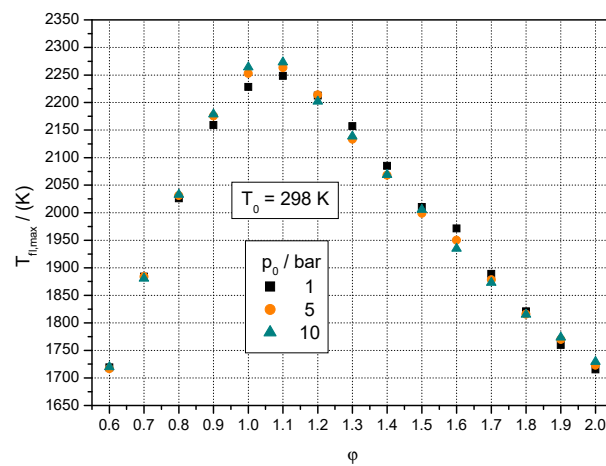


(c)

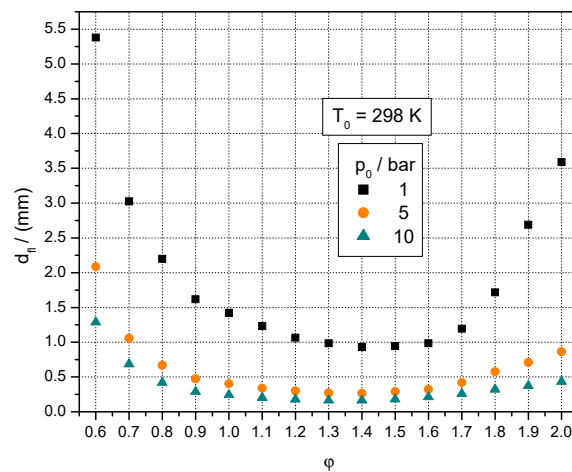
**Figure 1.** The influence of initial temperature,  $T_0$ , and equivalence ratio,  $\phi$ , on: (a) laminar burning velocities,  $S_u$ , (b) flame temperature,  $T_{fl,max}$ , and (c) flame front thickness,  $d_{fl}$ , of multifuel A with air at  $p_0 = 1$  bar.



(a)



(b)



(c)

**Figure 2.** The influence of initial pressure,  $p_0$ , and equivalence ratio,  $\phi$ , on: (a) laminar burning velocities,  $S_u$ , (b) flame temperature,  $T_{fl,max}$ , and (c) flame front thickness,  $d_{fl}$ , of multifuel A with air at  $T_0 = 298$  K.

The burning velocities obtained for flames at higher initial pressures and temperatures are given in Figure 3 ( $\varphi = 0.9\text{--}1.0$ ) vs. the initial temperatures at various initial pressures ( $p_0$ : 1–20 bar) and in Figure 4 ( $\varphi = 1.0$ ) vs. the initial pressures at various initial temperatures ( $T_0$ : 298–450 K).

The lines in Figures 3 and 4 are the best-fit correlations of the computed burning velocities with the initial pressure or temperature. The burning velocities decrease with the initial pressure increase and increase when the initial temperature increases.

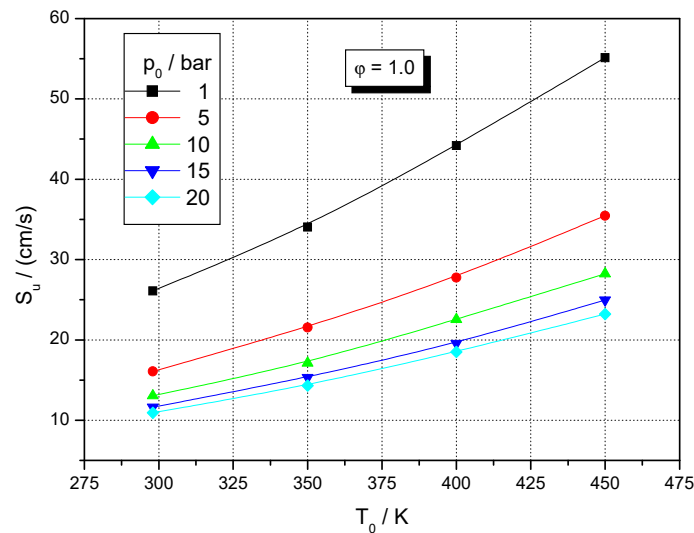


**Figure 3.** Computed burning velocities of *multifuel A* with air mixtures, for 24.7% *multifuel A* concentrations ( $\varphi = 1.0$ ), vs. the initial temperature, at various initial pressures ( $p_0$ : 1–20 bar).

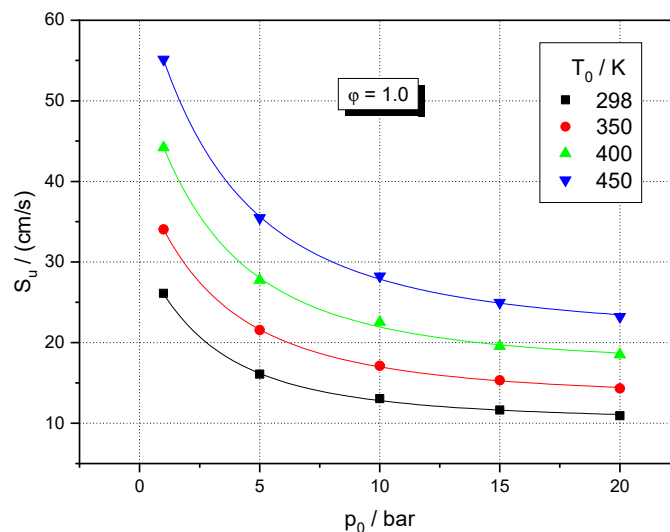


**Figure 4.** Computed burning velocities of stoichiometric *multifuel A* with air mixture (24.73% or  $\varphi = 1.0$ ) vs. the initial pressure, at various initial temperatures ( $T_0$ : 298–450 K).

The dependence of  $S_u$  on the initial pressure of fuel-oxidant mixtures can be described quantitatively in the form of a power law; thereby, the data were analyzed according to the following empirical equation [38,39]:

$$S_u = S_{u,ref} \left( \frac{p}{p_{ref}} \right)^\beta \quad (2)$$

where  $S_{u,ref}$  is the normal burning velocity at  $p_{ref}$ , the reference pressure, and  $\beta$  is the baric coefficient. Choosing  $p_{ref} = 1$  bar as the reference pressure, the baric coefficients of normal burning velocities for mixtures of *multifuel A* with air with different concentrations were calculated by a non-linear regression analysis of  $S_u = f(p)$  data. Some values that are characteristic of these mixtures at various initial temperatures are given in Table 1. The baric coefficients of normal burning velocities for *multifuel A* with air mixtures at different  $T_0$  ( $T_0$ : 298 K, 350 K, 400 K) have values within the range  $-0.283, \dots, -0.385$ . The usual values from the literature for the baric coefficient,  $\beta$ , are between  $-0.500$  and  $-0.120$  for single fuel–air mixtures at 300 K [39–43].

**Table 1.** Baric coefficients ( $-\beta$ ) of normal burning velocities for mixtures of *multifuel A* with air at various equivalence ratios ( $\varphi$ : 0.7–1.6) and different initial temperatures.

$T_0$ (K)	298	350	400
$\varphi$			
0.7	$0.385 \pm 0.002$	$0.374 \pm 0.014$	$0.360 \pm 0.007$
0.8	$0.334 \pm 0.006$	$0.352 \pm 0.002$	$0.331 \pm 0.003$
0.9	$0.311 \pm 0.007$	$0.312 \pm 0.003$	$0.317 \pm 0.009$
1.0	$0.301 \pm 0.001$	$0.293 \pm 0.009$	$0.291 \pm 0.002$
1.1	$0.289 \pm 0.007$	$0.285 \pm 0.007$	$0.283 \pm 0.008$
1.2	$0.300 \pm 0.005$	$0.289 \pm 0.019$	$0.283 \pm 0.014$
1.3	$0.303 \pm 0.012$	$0.304 \pm 0.011$	$0.291 \pm 0.007$
1.4	$0.328 \pm 0.013$	$0.323 \pm 0.023$	$0.323 \pm 0.023$
1.5	$0.349 \pm 0.007$	$0.342 \pm 0.031$	$0.319 \pm 0.023$
1.6	$0.415 \pm 0.011$	$0.368 \pm 0.019$	$0.345 \pm 0.013$

Similarly, the dependence of  $S_u$  on the initial temperature of fuel–oxidant mixtures has the form [40,44,45]:

$$S_u = S_{u,ref} \left( \frac{T}{T_{ref}} \right)^\alpha \quad (3)$$

where  $S_{u,ref}$  is the normal burning velocity at  $T_{ref}$ , the reference temperature, and  $\alpha$  is the thermal coefficient. Using the ambient temperature as the reference, the thermal coefficients,  $\alpha$ , of normal burning velocities for *multifuel A* with air mixtures were calculated by a non-linear regression analysis of  $S_u = f(T)$  data. Some values that are characteristic of the examined *multifuel A* with air at various initial pressures are given in Table 2. The thermal coefficients at  $p_0 = 1$  bar range from 1.66 to 2.31, values within the domain characteristic of hydrocarbon–air mixtures. The usual values for the thermal coefficient  $\alpha$  of  $S_u$  for fuel–air mixtures at 1 bar are between 1.50 and 2.40 [42,43,46,47].

**Table 2.** Thermal coefficients ( $\alpha$ ) of normal burning velocities for mixtures of *multifuel A* with air at various equivalence ratios ( $\varphi$ : 0.70–1.60) and different initial pressures.

$p_0$ (bar)	1	5	10
$\varphi$			
0.7	$2.107 \pm 0.013$	$2.245 \pm 0.096$	$2.309 \pm 0.026$
0.8	$2.018 \pm 0.102$	$2.035 \pm 0.051$	$2.137 \pm 0.065$
0.9	$1.933 \pm 0.043$	$1.913 \pm 0.065$	$1.862 \pm 0.008$
1.0	$1.811 \pm 0.089$	$1.861 \pm 0.023$	$1.886 \pm 0.111$
1.1	$1.754 \pm 0.042$	$1.753 \pm 0.020$	$1.739 \pm 0.005$
1.2	$1.652 \pm 0.021$	$1.779 \pm 0.047$	$1.759 \pm 0.054$
1.3	$1.696 \pm 0.024$	$1.742 \pm 0.015$	$1.829 \pm 0.050$
1.4	$1.745 \pm 0.001$	$1.827 \pm 0.039$	$1.878 \pm 0.080$
1.5	$1.704 \pm 0.077$	$1.937 \pm 0.115$	$1.907 \pm 0.112$
1.6	$1.661 \pm 0.135$	$2.033 \pm 0.038$	$2.210 \pm 0.107$

Both the baric and thermal coefficients depend on the composition of the fuel–oxidant mixtures and on the range of pressures and initial temperatures for which they are determined.

From the variation in the burning velocities against the initial pressure and temperature, the overall kinetic parameters (apparent activation energy and overall reaction order) of the combustion reaction can be determined [39,40,45,48]. These global kinetic parameters are of importance in the CFD (Computational Fluid Dynamics) modeling of explosion propagation under various confinement conditions.

The variation in the calculated burning velocities with the total initial pressure and temperature of *multifuel A*–air flames afforded the determination of the overall activation parameters of the *multifuel*–oxygen reaction occurring under flame conditions. The overall reaction orders,  $n$ , were determined from the baric coefficients,  $\beta$ , of the calculated burning velocities according to the following equation [49]:

$$n = 2(\beta + 1) \quad (4)$$

The overall activation energies,  $E_a$ , of the *multifuel A* reaction with oxygen under flame conditions were determined according to the following equation [48]:

$$\ln S_u = \text{const} - \frac{E_a}{2R\overline{T_{f,p}}} \quad (5)$$

where  $\overline{T_{f,p}}$  is the average temperature in the flame front, computed by means of the adiabatic flame temperatures of the isobaric combustion  $T_{f,p}$  [48] as:

$$T_{f,av} = T_0 + 0.74(T_f - T_0) \quad (6)$$

The plots of the computed laminar burning velocities versus the reciprocal adiabatic flame temperatures of stoichiometric *multifuel A* with air mixture (24.73% or  $\phi = 1.0$ ) are given in Figure 5. The slopes of the linear correlations gave the overall activation energies.

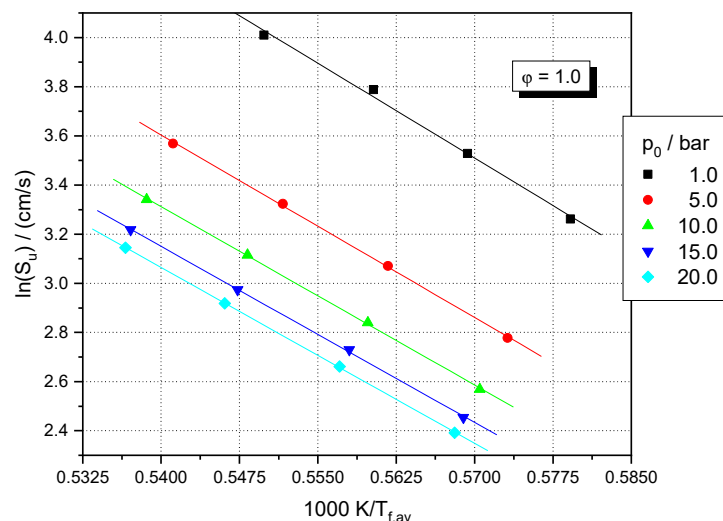


**Figure 5.** Computed laminar burning velocities vs. the reciprocal adiabatic flame temperatures of stoichiometric *multifuel A* with air mixture (24.73% or  $\phi = 1.0$ ). Each dataset contains results computed at various initial temperatures and various initial pressures ( $p_0$ : 1–20 bar).

The results characteristic of the studied mixtures of *multifuel A* with air are given in Tables 3 and 4.

The overall reaction orders are only slightly influenced by the initial temperature; they range between 1.23 and 1.43, similar to those of other gaseous fuel–air mixtures: ethylene [50], ethane [45], and propene [51].

Table 4 shows the values of the apparent activation energies of the *multifuel A* with air at different equivalence ratios between  $\varphi$ : 0.70 and 1.60. It is observed that the overall activation energy ranges between 257 and 428 kJ/mol for variable initial pressures between 1 and 10 bar and variable equivalence ratios between  $\varphi$ : 0.70 and 1.60.

**Table 3.** Overall reaction orders,  $n$ , of *multifuel A* with air mixture at various equivalence ratios ( $\varphi$ : 0.70–1.60) and various initial temperatures ( $T_0$ : 298 K, 350 K, 400 K).

$T_0$ (K)	$n$										
	$\varphi$	0.70	0.80	0.90	1.00	1.10	1.20	1.30	1.40	1.50	1.60
298 K		1.23	1.33	1.38	1.40	1.42	1.40	1.39	1.34	1.30	1.17
350 K		1.25	1.30	1.38	1.41	1.43	1.42	1.39	1.35	1.32	1.26
400 K		1.28	1.34	1.37	1.42	1.43	1.43	1.42	1.35	1.36	1.31

**Table 4.** Overall activation energies,  $E_a$ , of *multifuel A* with air mixture at various equivalence ratios ( $\varphi$ : 0.70–1.60) and various initial pressures ( $p_0$ : 1 bar, 5 bar, 10 bar).

$p_0$ (bar)	$E_a$ (kJ/mol)										
	$\varphi$	0.70	0.80	0.90	1.00	1.10	1.20	1.30	1.40	1.50	1.60
1 bar		290	335	374	428	386	339	284	249	258	300
5 bar		304	338	363	412	372	365	306	282	277	311
10 bar		300	329	365	402	384	311	249	302	310	300

Figures 6 and 7 present the sum of the computed peak mass fractions of several reactive species (H, OH, O, HO<sub>2</sub>, CH<sub>2</sub>O) in the flame front of the stoichiometric *multifuel A* with air mixture (24.73% or  $\varphi = 1.0$ ) vs. the initial temperature at various initial pressures (1 bar, 5 bar, and 10 bar) (Figure 6) and vs. the initial pressure at various initial temperatures (298 K, 400 K, and 500 K) (Figure 7). It is observed that, if the initial temperature increases, then the sum of the peak mass fractions of the examined reactive species in the front increases (Figure 6), while if the initial pressure increases, the sum of the peak mass fractions of these species decreases (Figure 7).

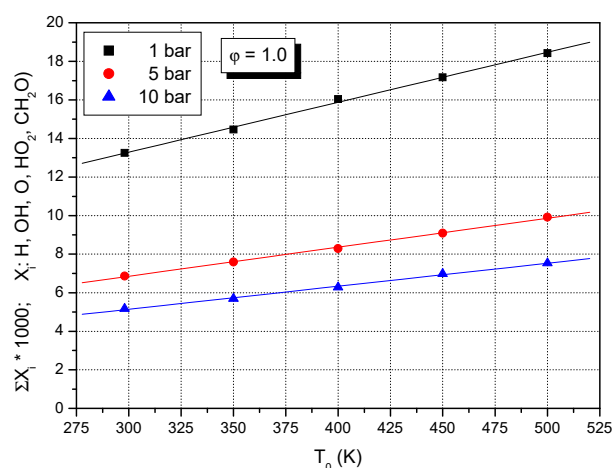


**Figure 6.** The sum of the peak mass fractions for several reactive species in the flame front of the stoichiometric *multifuel A* with air mixture (24.73% or  $\varphi = 1.0$ ) vs. the initial temperature, at various initial pressures (1 bar, 5 bar, and 10 bar).

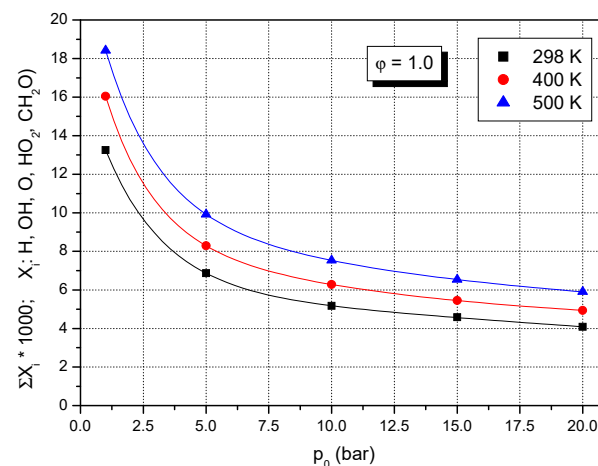


**Figure 7.** The sum of peak mass fractions for several reactive species in the flame front of the stoichiometric *multifuel A* with air mixture (24.73% or  $\phi = 1.0$ ) vs. the initial pressure, at various initial temperatures (298 K, 400 K, and 500 K).

The variations found for the sum of the peak mass fractions of reactive species against temperature or pressure explain the variations observed for the laminar burning velocities against the temperature or pressure of the unburned mixture, reflecting the variations in the reactivity of the examined pyrolysis gas.

The topic of the present paper covers a missing gap in the field, which is the characterization of complex flammable mixtures, formed by *multifuels* and air. In recent decades, the study of alternative and clean fuels has attracted increasing attention with the depletion of fossil fuels and the strengthening of pollutant emission regulations. One of the prospective alternative fuels is the *multifuel* mixture. Such mixture, obtained from renewable sources (biomass), is recognized as one of the most promising alternative fuels. The *multifuel* mixture could be utilized in specific energy devices, such as industry gas turbines and gas engines operated at high pressures and temperatures. Still, such mixtures are poorly characterized, especially from the point of view of combustion with air, at various initial pressures and temperatures. The paper delivers the laminar burning velocities of a *multifuel*–air mixture in these various initial conditions. As a fundamental property for fuel combustion in practical energy devices, the laminar burning velocity is determined by the combined properties of the diffusivity, exothermicity, and reactivity of a fuel. The laminar burning velocity is a key parameter for describing the flame stabilization, extinction limits, flame structures, and velocity.

#### 4. Conclusions

The aim of the present paper was the numerical investigation of flame propagation in the flammable gas-phase mixture of *multifuel A* with air, the *multifuel A* being obtained by the pyrolysis of willow wood in an inert atmosphere at 800 °C. The *multifuel A* composition (by volume) is: 38.20% CO/21.87% H<sub>2</sub>/17.44% CH<sub>4</sub>/1.15% O<sub>2</sub>/17.15% CO<sub>2</sub>/4.19% N<sub>2</sub>. The propagation of the free laminar premixed flames of *multifuel A* with air was examined at initial temperatures between 298 and 500 K, initial pressures between 1 and 20 bar, and fuel equivalence ratios between 0.6 and 2.0. The numerical simulation of these flames used the package INSFLA designed for free laminar premixed flames. The laminar burning velocities,  $S_{fl}$ , maximum flame temperature,  $T_{fl,max}$ , flame front thickness,  $d_f$ , and peak concentrations of the main reaction intermediates were investigated and discussed. Based on the correlations of laminar burning velocities with the initial pressure and temperature, the overall activation parameters (overall activation energy and overall reaction order) of *multifuel A* oxidation with air were reported.

The obtained results could have an impact on the practical use of gaseous products generated from willow wood pyrolysis, since they reveal the influence of operational

parameters (initial pressure and initial temperature) on the laminar burning velocity, which in turn influences the rate of heat release and the composition of burned gases.

The examination of the results delivered the following concluding remarks:

- The influence of process parameters (initial pressure and temperature) on the laminar burning velocities of *multifuel A* mixed with air in various mixtures can be expressed as power law equations, providing a method for modeling these processes. In these equations, the thermal and baric coefficients ( $\alpha$  and  $\beta$ ) of burning velocities correspond to values that are usually characteristic of light hydrocarbons.
- The correlation between the laminar burning velocities of preheated *multifuel A* with the various air mixtures and the average flame temperature allowed for the determination of the overall activation energy. Likewise, the mathematical relationship determined between the combustion velocities and initial pressure of these mixtures at a constant initial temperature allowed for the determination of overall reaction orders. These global parameters (activation energy and reaction orders) provide valuable input data for Computational Fluid Dynamics (CFD) modeling and simulations of flame propagation under various conditions.
- The observed effects of process parameters (initial temperature and pressure) on the maximum flame temperature, the thickness of the flame, and the peak concentrations of main reaction intermediates provide valuable insight into how these parameters affect laminar burning velocities.
- The concentrations of the most important radical species in the flame front that take part in intermediate reactions under the variable initial conditions of pressure, temperature, and concentration were presented. Knowledge of radical species concentrations and of flame adiabatic temperatures, along with the determination of burning velocities, is important because they afford the comparison of experimental data with the predictions of the kinetic scheme.

Future studies should request measurements of the laminar burning velocities of *multifuel A* with air mixtures, which are necessary to validate the computed data from the present paper.

**Author Contributions:** Conceptualization, M.M.; methodology, M.M.; software, M.M. and D.R.; validation, D.R., D.B. and C.M.; formal analysis, D.R.; investigation, D.B. and C.M.; resources, D.B. and C.M.; data curation, M.M. and D.R.; writing—original draft preparation, M.M. and D.R.; writing—review and editing, M.M., D.R., D.B. and C.M.; visualization, M.M.; supervision, D.R. and C.M.; project administration, D.B. and C.M.; funding acquisition, D.B. and C.M. All authors have read and agreed to the published version of the manuscript.

**Funding:** This research was partly funded by Romania's "Competitiveness Operational Programme 2014–2020" Priority Axis 1: Research, Technological Development, and Innovation (RD&I) to Support Economic Competitiveness and Business Development Action 1.1.4. Attracting high-level personnel from abroad in order to enhance the RD capacity ID/Cod My SMIS: P\_37\_768/103651; No. Contract: 39/02.09.2016 and by the Romanian Academy under the research project "Dynamics of fast oxidation and decomposition reactions in homogeneous systems" of the "Ilie Murgulescu" Institute of Physical Chemistry—Bucharest. Partial support was provided by the USDA NIFA Hatch Program (LAB #94443).

**Data Availability Statement:** Not applicable.

**Acknowledgments:** The authors gratefully thank Ulrich Maas (Institut für Technische Verbrennung, Karlsruhe, Germany) and Detlev Markus (Physikalisch-Technische Bundesanstalt, Braunschweig, Germany) for the permission to run the program INSFLA and for the provided assistance. The paper is published with the approval of the Director of the Louisiana Agricultural Experiment Station as manuscript #2023-232-38925.

**Conflicts of Interest:** The authors declare no conflict of interest.

## References

1. Basu, P. *Biomass Gasification and Pyrolysis: Practical Design and Theory*; Academic Press: Cambridge, MA, USA, 2010.
2. Pio, G.; Salzano, E. Laminar burning velocity of multi-component gaseous mixtures. *Chem. Eng. Trans.* **2018**, *67*, 1–6.
3. Gu, X.J.; Haq, M.Z.; Lawes, M.; Woolley, R. Laminar burning velocity and Markstein lengths of methane–air mixtures. *Combust. Flame* **2000**, *121*, 41–58. [[CrossRef](#)]
4. Mitu, M.; Giurcan, V.; Razus, D.; Oancea, D. Inert gas influence on the laminar burning velocity of methane–air mixtures. *J. Hazard. Mater.* **2017**, *321*, 440–448. [[CrossRef](#)] [[PubMed](#)]
5. Zhang, Q.; Yu, Y.; Li, Y.; Chen, Z.; Jiang, J. Coupling effects of venting and inerting on explosions in interconnected vessels. *J. Loss Prev. Process. Ind.* **2020**, *65*, 104132. [[CrossRef](#)]
6. Halter, F.; Chauveau, C.; Djebaili-Chaumeix, N.; Gökalp, I. Characterization of the effects of pressure and hydrogen concentration on laminar burning velocities of methane–hydrogen–air mixtures. *Proc. Combust. Inst.* **2005**, *30*, 201–208. [[CrossRef](#)]
7. Brower, M.; Petersen, E.L.; Metcalfe, W.; Curran, H.J.; Furi, M.; Bourque, G.; Aluri, N.; Güthe, F. Ignition Delay Time and Laminar Flame Speed Calculations for Natural Gas/Hydrogen Blends at Elevated Pressures. *J. Eng. Gas Turbines Power* **2013**, *135*, 021504. [[CrossRef](#)]
8. Mitu, M.; Razus, D.; Schroeder, V. Laminar Burning Velocities of Hydrogen-Blended Methane–Air and Natural Gas–Air Mixtures, Calculated from the Early Stage of  $p(t)$  Records in a Spherical Vessel. *Energies* **2021**, *14*, 7556. [[CrossRef](#)]
9. Luo, Z.; Li, R.; Wang, T.; Cheng, F.; Liu, Y.; Yu, Z.; Fan, S.; Zhu, X. Explosion pressure and flame characteristics of CO/CH<sub>4</sub>/air mixtures at elevated initial temperatures. *Fuel* **2020**, *268*, 117377. [[CrossRef](#)]
10. Natarajan, J.; Lieuwen, T.; Seitzman, J. Laminar flame speeds of H<sub>2</sub>/CO mixtures: Effect of CO<sub>2</sub> dilution, preheat temperature, and pressure. *Combust. Flame* **2007**, *151*, 104–119. [[CrossRef](#)]
11. Bouvet, N.; Chauveau, C.; Gökalp, I.; Lee, S.-Y.; Santoro, R. Characterization of syngas laminar flames using the Bunsen burner configuration. *Int. J. Hydrogen Energy* **2011**, *36*, 992–1005. [[CrossRef](#)]
12. Burbano, H.J.; Pareja, J.; Amell, A.A. Laminar burning velocities and flame stability analysis of H<sub>2</sub>/CO/air mixtures with dilution of N<sub>2</sub> and CO<sub>2</sub>. *Int. J. Hydrogen Energy* **2011**, *36*, 3232–3242. [[CrossRef](#)]
13. Li, H.-M.; Li, G.-X.; Jiang, Y.-H. Laminar burning velocities and flame instabilities of diluted H<sub>2</sub>/CO/air mixtures under different hydrogen fractions. *Int. J. Hydrogen Energy* **2018**, *43*, 16344–16354. [[CrossRef](#)]
14. Prathap, C.; Ray, A.; Ravi, M. Investigation of nitrogen dilution effects on the laminar burning velocity and flame stability of syngas fuel at atmospheric condition. *Combust. Flame* **2008**, *155*, 145–160. [[CrossRef](#)]
15. Cheng, T.S.; Chang, Y.C.; Chao, Y.C.; Chen, G.B.; Li, Y.H.; Wu, C.Y. An experimental and numerical study on characteristics of laminar premixed H<sub>2</sub>/CO/CH<sub>4</sub>/air flames. *Int. J. Hydrogen Energy* **2011**, *36*, 13207–13217. [[CrossRef](#)]
16. Varghese, R.J.; Kumar, S. Laminar burning velocities of LCV syngas–air mixtures at high temperature and pressure conditions. *Fuel* **2020**, *279*, 118475. [[CrossRef](#)]
17. Oliveira, G.P.; Sbampato, M.E.; Martins, C.A.; Santos, L.R.; Barreta, L.G.; Gonçalves, R.F.B. Experimental laminar burning velocity of syngas from fixed-bed downdraft biomass gasifiers. *Renew. Energy* **2020**, *153*, 1251–1260. [[CrossRef](#)]
18. Di Benedetto, A.; Di Sarli, V.; Salzano, E.; Cammarota, F.; Russo, G. Explosion behavior of CH<sub>4</sub>/O<sub>2</sub>/N<sub>2</sub>/CO<sub>2</sub> and H<sub>2</sub>/O<sub>2</sub>/N<sub>2</sub>/CO<sub>2</sub> mixtures. *Int. J. Hydrogen Energy* **2009**, *34*, 6970–6978. [[CrossRef](#)]
19. Kobayashi, H.; Otawara, Y.; Wang, J.; Matsuno, F.; Ogami, Y.; Okuyama, M.; Kudo, T.; Kadowaki, S. Turbulent premixed flame characteristics of a CO/H<sub>2</sub>/O<sub>2</sub> mixture highly diluted with CO<sub>2</sub> in a high-pressure environment. *Proc. Combust. Inst.* **2013**, *34*, 1437–1445. [[CrossRef](#)]
20. Basco, A.; Cammarota, F.; Di Sarli, V.; Salzano, E.; Di Benedetto, A. Theoretical analysis of anomalous explosion behavior for H<sub>2</sub>/CO/O<sub>2</sub>/N<sub>2</sub> and CH<sub>4</sub>/O<sub>2</sub>/N<sub>2</sub>/CO<sub>2</sub> mixtures in the light of combustion-induced rapid phase transition. *Inter-Natl. J. Hydrog. Energy* **2015**, *40*, 8239–8247. [[CrossRef](#)]
21. Francisco, R.W., Jr.; Oliveira, A.A.M. Measurement of the adiabatic flame speed and overall activation energy of a methane enriched H<sub>2</sub>/CO/CO<sub>2</sub>/N<sub>2</sub> low heating value mixture. *Int. J. Hydrogen Energy* **2020**, *45*, 29533–29545. [[CrossRef](#)]
22. Zhang, Q.; Chen, G.; Deng, H.; Wen, X.; Wang, F.; Zhang, A.; Sheng, W. Experimental and numerical study of the effects of oxygen-enriched air on the laminar burning characteristics of biomass-derived syngas. *Fuel* **2021**, *285*, 119183. [[CrossRef](#)]
23. Sittisun, P.; Tippayawong, N. Characterization of laminar premixed flame firing biomass derived syngas with oxygen enriched air. *Int. J. Smart Grid Clean Energy* **2019**, *8*, 702–709. [[CrossRef](#)]
24. Xu, C.; Zhong, A.; Li, X.; Wang, C.; Sahu, A.; Xu, H.; Lattimore, T.; Zhou, K.; Huang, Y. Laminar burning characteristics of upgraded biomass pyrolysis fuel derived from rice husk at elevated pressures and temperatures. *Fuel* **2017**, *210*, 249–261. [[CrossRef](#)]
25. Xu, C.; Wang, H.; Oppong, F.; Li, X.; Zhou, K.; Zhou, W.; Wu, S.; Wang, C. Determination of laminar burning characteristics of a surrogate for a pyrolysis fuel using constant volume method. *Energy* **2020**, *190*, 116315. [[CrossRef](#)]
26. Zhou, Q.; Cheung, C.; Leung, C.; Li, X.; Li, X.; Huang, Z. Effects of fuel composition and initial pressure on laminar flame speed of H<sub>2</sub>/CO/CH<sub>4</sub> bio-syngas. *Fuel* **2019**, *238*, 149–158. [[CrossRef](#)]
27. Huang, Z.; Zhang, Y.; Zeng, K.; Liu, B.; Wang, Q.; Jiang, D. Measurements of laminar burning velocities for natural gas–hydrogen–air mixtures. *Combust. Flame* **2006**, *146*, 302–311. [[CrossRef](#)]
28. Tahtouh, T.; Halter, F.; Samson, E.; Mounaim-Rousselle, C. Effects of hydrogen addition and nitrogen dilution on the laminar flame characteristics of premixed methane–air flames. *Int. J. Hydrogen Energy* **2009**, *34*, 8329–8338. [[CrossRef](#)]

29. Law, C.; Kwon, O. Effects of hydrocarbon substitution on atmospheric hydrogen–air flame propagation. *Int. J. Hydrogen Energy* **2004**, *29*, 867–879. [[CrossRef](#)]
30. Qiao, L.; Gu, Y.; Dahm, W.; Oran, E.; Faeth, G. A study of the effects of diluents on near-limit H<sub>2</sub>–air flames in microgravity at normal and reduced pressures. *Combust. Flame* **2007**, *151*, 196–208. [[CrossRef](#)]
31. Salzano, E.; Basco, A.; Cammarota, F.; Di Sarli, V.; Di Benedetto, A. Explosions of syngas/CO<sub>2</sub> mixtures in oxy-gen-enriched air. *Ind. Eng. Chem. Res.* **2012**, *51*, 7671–7678. [[CrossRef](#)]
32. Ionescu, G.; Bulmau, C.; Mărculescu, C. Bio-Gaseous Fuels from Agricultural Waste Pyrolysis (Part I). *MATEC Web Conf.* **2019**, *290*, 11004. [[CrossRef](#)]
33. Maas, U.; Warnatz, J. Ignition processes in hydrogen–oxygen mixtures. *Combust. Flame* **1978**, *74*, 53–69. [[CrossRef](#)]
34. Warnatz, J.; Maas, U.; Dibble, R. *Combustion*, 3rd ed.; Springer: Berlin/Heidelberg, Germany; New York, NY, USA, 2001.
35. Warnatz, J. The structure of laminar alkane-, alkene-, and acetylene flames. In *Symposium (International) on Combustion*; The Combustion Institute: Pittsburgh, PA, USA, 1981; pp. 369–384.
36. Heghes, C.I. C1–C4 Hydrocarbon Oxidation Mechanism. Ph.D. Thesis, Heidelberg University, Heidelberg, Germany, 2006.
37. Burcat, A. Thermochemical Data for Combustion Calculations. In *Combustion Chemistry*; Gardiner, W.C., Jr., Ed.; Springer: New York, NY, USA; Berlin, Germany; Tokyo, Japan, 1984; pp. 455–473. [[CrossRef](#)]
38. Van Tiggelen, A.; Balaceanu, J.; Burger, J.; de Soete, G.; Sajus, L.; Sale, B.; van Tiggelen, P. *Oxidations et Combustions*; Technip: Paris, France, 1968; Volume I.
39. Lewis, B.; von Elbe, G. *Combustion, Flames and Explosion of Gases*, 3rd ed.; Academic Press: New York, NY, USA; London, UK, 1987.
40. Khitrin, L.N. *The Physics of Combustion and Explosion: (Fizika Gorennya i Vzryva)*; Israel Program for Scientific Translations: Israel, Jerusalem, 1962; Volume 61.
41. Babkin, V.S.; Kozachenko, L.S. Study of normal burning velocity in methane-air mixtures at high pressures. *Combust. Explos. Shock. Waves* **1966**, *2*, 46–52. [[CrossRef](#)]
42. Metghalchi, M.; Keck, J. Laminar burning velocity of propane-air mixtures at high temperature and pressure. *Combust. Flame* **1980**, *38*, 143–154. [[CrossRef](#)]
43. Konnov, A.A. The temperature and pressure dependences of the laminar burning velocity: Experiments and modelling. In Proceedings of the 7th Proceedings of the European Combustion Meeting—2015, Budapest, Hungary, 30 March–2 April 2015.
44. Carloganu, C. *Combustii Rapide în Gaze și Pulberi*; Cap. 1 și 2; Tehnica: Bucuresti, Romania, 1986.
45. Mitu, M.; Razus, D.; Giurcan, V.; Oancea, D. Normal burning velocity and propagation speed of ethane–air: Pressure and temperature dependence. *Fuel* **2015**, *147*, 27–34. [[CrossRef](#)]
46. Andrews, G.; Bradley, D. Determination of burning velocities: A critical review. *Combust. Flame* **1972**, *18*, 133–153. [[CrossRef](#)]
47. Glassman, I.; Yetter, R. *Combustion*, 4th ed.; Elsevier: Amsterdam, The Netherlands, 2008.
48. Burke, R.; Dewael, F.; Van Tiggelen, A. Kinetics of the propylene—Oxygen flame reaction. *Combust. Flame* **1963**, *7*, 83–87. [[CrossRef](#)]
49. Potter, A.; Berlad, A. The effect of fuel type and pressure on flame quenching. *Symp. Combust.* **1957**, *6*, 27–36. [[CrossRef](#)]
50. Movileanu, C.; Razus, D.; Oancea, D. Additive Effects on the Burning Velocity of Ethylene—Air Mixtures. *Energy Fuels* **2011**, *25*, 2444–2451. [[CrossRef](#)]
51. Razus, D.; Oancea, D.; Ionescu, N.I. Burning velocity determination by spherical bomb technique. II. Propylene–air mixtures of various compositions, pressures and temperatures. *Rev. Roum. Chim.* **2000**, *45*, 319–330.

**Disclaimer/Publisher’s Note:** The statements, opinions and data contained in all publications are solely those of the individual author(s) and contributor(s) and not of MDPI and/or the editor(s). MDPI and/or the editor(s) disclaim responsibility for any injury to people or property resulting from any ideas, methods, instructions or products referred to in the content.